

Formation of nanocrystalline phases in the Cu–Zn system during mechanical alloying

S. K. PABI, J. JOARDAR, B. S. MURTY

Department of Metallurgical and Materials Engineering, Indian Institute of Technology, Kharagpur 721 302, India

The evolution of various nanocrystalline phases in the Cu–Zn system during the course of mechanical alloying of elemental powder blends, manifests a similar sequence of phase formation in all the compositions. Zinc-rich phases were always first to form, which can be attributed to the diversities of diffusivities and diffusion distances in the constituents. The extent of zinc in α -phase becomes significant only after α turns nanocrystalline. The crystallite size of α reached a minimum (~ 18 nm) near the α – β phase boundary, while the β and ϵ phases showed quite coarse crystallite size due to their low melting points. Alloying was sluggish during dry milling compared to wet milling, or at lower milling speed, which demonstrates the effects of oxidation during milling and lower milling energy.

1. Introduction

The application of mechanical alloying (MA) to produce nanocrystalline alloys [1, 2] and to induce various phase transformations [3–5] has given a new dimension to the MA technology in recent years. In spite of considerable work on the production of stable and metastable phases [6, 7] and phase mixtures [6] by MA, the phase transformation in nanocrystalline materials during MA still remains a subject of immense interest. The phase formation seems to depend on various milling parameters apart from the nature of the system itself. The present work is an effort to understand the fundamentals of phase formation during the course of MA of Cu–Zn blends. The Cu–Zn system has been chosen in view of its known alloy chemistry.

In an earlier work on MA of equiatomic Cu–Zn blend [8], performed in a SPEX-8000 mixer mill, rapid alloying and the appearance of strain-induced cubic martensite followed by β brass formation have been reported. In another recent work [9] on MA of Cu–80 and 85 at % Zn composition using the SPEX 8000 mill, the role of milling atmosphere on phase transformation has been highlighted. However, neither of these works has reported nanocrystalline phase formation. In addition, the influence of various other milling parameters on the phase formation during MA in the Cu–Zn system has not been reported so far. In the present paper, nanocrystalline phase formation and the sequence of phase evolution in the Cu–Zn system during MA under different milling conditions have been studied in detail over a wide range of compositions.

2. Experimental procedure

Pure elemental Cu–Zn powder blends of -325 mesh size (≤ 45 μm) with nominal composition of $\text{Cu}_{100-x}\text{Zn}_x$ ($x = 15, 30, 40, 50, 65, 85$) were studied. MA was carried out in a Fritsch Pulverisette-5 planetary ball mill using a steel vial with steel balls. The ball to powder (B/P) weight ratio was 10:1 and the milling speed was 300 r.p.m., unless otherwise stated. WC medium and 200 r.p.m. were also employed in selected cases. Milling was done under wet as well as dry conditions. The phase analysis was carried out by means of X-ray diffraction (XRD) using Philips PW 1840 diffractometer with CuK_α radiation. Crystalline size was determined from the XRD peak broadening by applying Scherrer's formula after elimination of strain and instrumental broadening contributions [10, 11]. Change in solid solubility was estimated by comparing the copper peak shift with standard lattice parameter data [12]. Transmission electron microscopic (TEM) studies were performed in Philips CM 12 to confirm the nanocrystalline nature of the phases.

3. Results and discussion

3.1. Phase formation during MA

Nanocrystalline ϵ , γ , β and α phases were synthesized by MA. Zinc-rich phases were produced in the initial stages of the MA process irrespective of the composition chosen. For example, in Cu–15 at % Zn, the ϵ peaks were detected in the XRD pattern within 0.5 h wet milling (Fig. 1). At this stage, the crystallite size of copper was quite coarse (> 200 nm). Upon prolonged milling, more stable copper-rich phases formed, as is

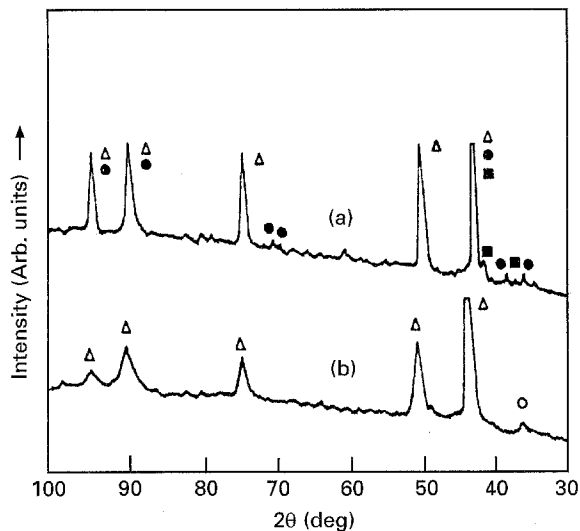


Figure 1 XRD patterns of Cu-15 at % Zn after (a) 0.5 h and (b) 4 h milling. (Δ) Cu, (●) Zn, (■) ϵ , (○) ZnO.

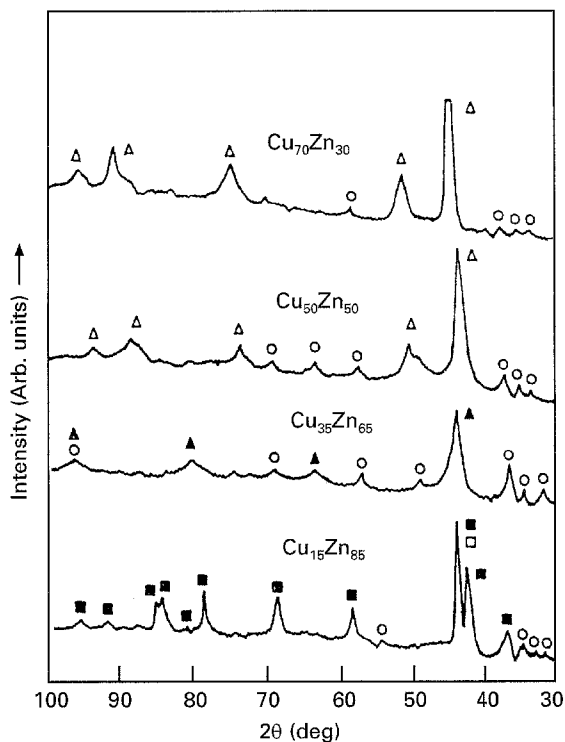


Figure 2 XRD patterns of different blends mechanically alloyed for 16 h. (Δ) Cu, (▲) β , (□) γ , (■) ϵ , (○) ZnO.

evident from Fig. 2. The early formation of zinc-rich phases in preference to copper-rich phases can be easily understood if one looks at the diffusivities of copper and zinc in each other. The probable limit of local temperature encountered during MA is $\sim 200^\circ\text{C}$, as evinced by the recent work on computer simulation [13, 14] and ball milling of Fe-C martensite [13]. The diffusivity of copper in zinc ($3.0 \times 10^{-18} \text{ m}^2 \text{ s}^{-1}$) at 200°C , extrapolated from high-temperature data [15], is about eight orders higher than that of zinc in copper ($8.2 \times 10^{-27} \text{ m}^2 \text{ s}^{-1}$). This can readily account for the early formation of zinc-rich phases when the grains are quite coarse. Based on the bulk diffusivities of constituents, a simple

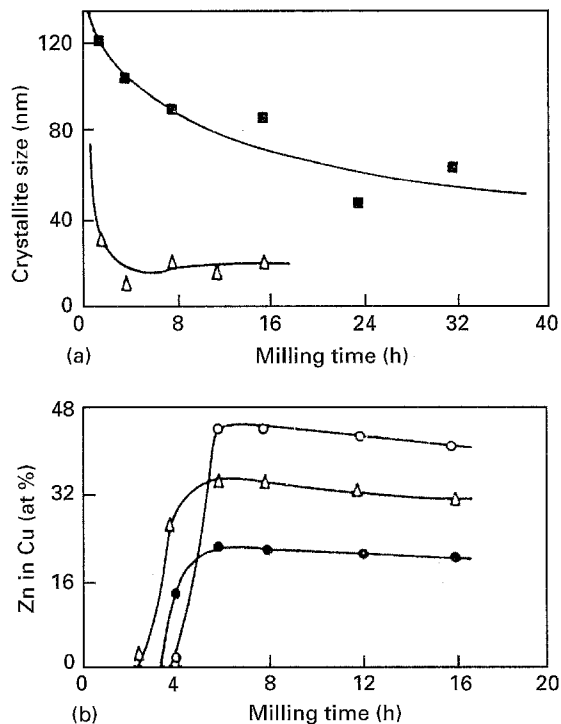


Figure 3 Change in (a) crystallite size and (b) zinc in copper-solid solution, as a function of milling time. (a) (■) ϵ , (Δ) α . (b) (○) $\text{Cu}_{50}\text{Zn}_{50}$, (Δ) $\text{Cu}_{60}\text{Zn}_{40}$, (●) $\text{Cu}_{70}\text{Zn}_{30}$.

estimate shows that the ϵ -phase formation would approach completion after about 2 h, if the initial diffusion field width in zinc is about 200 nm [16]. On the other hand, the present XRD results are evidence of a substantial presence of ϵ -phase within 0.5 h milling. This difference is expected, as ball milling induces a large density of dislocations that can enhance the alloying rate through short-circuit diffusion.

A sharp rise in the zinc content in the copper-rich α -solid solution was observed after α reached a crystallite size of about 15 nm (after ~ 4 h milling), as shown in Fig. 3a and b. The milling time and the crystallite size at which this fast enrichment of zinc in α occurred, was found to be quite insensitive to the composition of the elemental blend, up to 50 at % Zn. In these alloys, the maximum amount of zinc in α during the course of MA (Fig. 3b) increased with increasing zinc content of the elemental blend, as expected. A marginal extension of the α -phase field to ~ 44 at % Zn could be achieved in $\text{Cu}_{50}\text{Zn}_{50}$ blend. A gradual decrease of zinc in α was observed after milling beyond 8 h, which was associated with the formation of ZnO.

At nominal compositions of 65 and 80 at % Zn, β and ($\gamma + \epsilon$), respectively, were present after prolonged (~ 40 h) milling, while the equilibrium phase diagram predicts single-phase γ and ϵ formation at these compositions. In fact, as the milling of these two blends is continued beyond 8 h, the formation of copper-rich phases was found to be associated with the oxidation of zinc-rich phases. A similar observation is reported in a recent work [9] on elemental blends of Cu-80 and 85 at % Zn. However, for nominal compositions of 50 at % Zn or less, the copper-rich phases were found to form by destabilization of zinc-rich

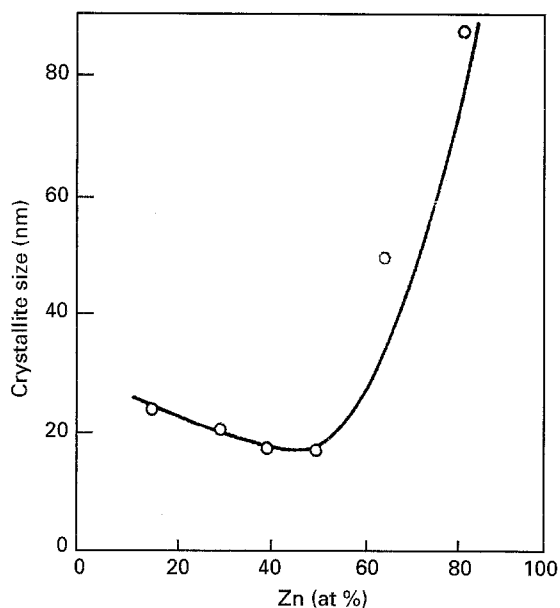


Figure 4 The crystallite size at different compositions after 16 h milling.

phases. The ZnO formation in these alloys becomes significant at a much later stage.

The crystallite size of zinc-rich ϵ phase decreased at a very slow rate with increasing milling time when compared to α phase (Fig. 3a). For instance, after 40 h milling, the crystallite size of ϵ phase was about 40 nm, while the α phase reached a crystallite size of ~ 15 nm within 4 h milling. This difference could be attributed to the difference in the melting points of the α and ϵ phases [17,18], because the tendency for cold welding in the case of low melting phases is expected to be more. Among the different compositions studied, the crystallite size is found to reach a minimum (~ 18 nm) in the α -phase at the phase boundary of α and β (Fig. 4). A similar result has been reported earlier [4] in the Ni–Al system at the phase boundary of NiAl and Ni₃Al. It is also interesting to note that no such minimum is observed at the γ and ϵ phase boundary. These results probably suggest that the nanocrystalline mixtures of only the high melting phases mutually hinder the coalescence of crystallites.

The nanocrystalline nature of the alloys obtained by MA was confirmed by TEM studies. The crystallite size of α phase observed by TEM (Fig. 5) in Cu₅₀Zn₅₀ blend seems to be in good agreement with the average size of ~ 18 nm as measured by XRD. The selected-area electron diffraction pattern (inset of Fig. 5) corresponds to the α phase, and shows no evidence of amorphization.

3.2. Effect of milling parameters

3.2.1. Milling atmosphere

A profound role of milling atmosphere on phase formation was evident from the dry and wet milling studies. While rapid alloying was observed on wet milling of Cu₇₀Zn₃₀, dry milling resulted only in oxide formation and no alloying could be detected even after 16 h milling. In Cu₅₀Zn₅₀, the formation of alloy

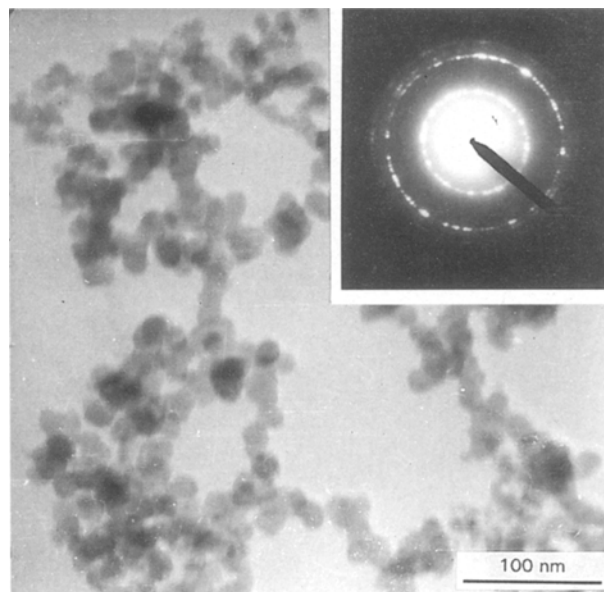


Figure 5 TEM bright-field image of α in Cu₅₀Zn₅₀ milled for 16 h. Inset is the selected-area diffraction pattern of the phase.

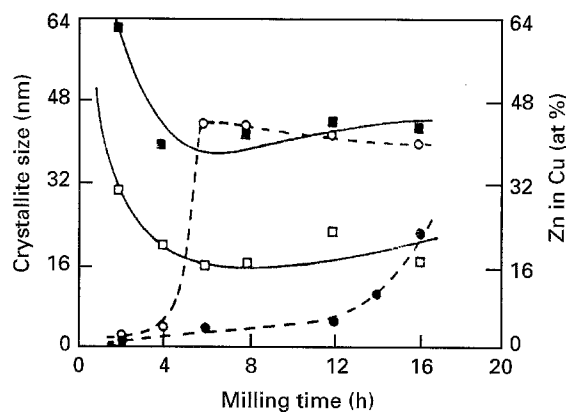


Figure 6 Time modulation of (\square , \blacksquare) crystallite size (—) and (\bullet , \circ) zinc in copper-solid solution (---) during (\blacksquare , \bullet) dry and (\square , \circ) wet milling of Cu₅₀Zn₅₀ blend.

phases was observed both in dry and wet milling conditions. During wet milling, however, a much more rapid crystallite size reduction and alloying (Fig. 6) were achieved as compared to dry milling for this composition. The sluggish rate of alloying in the dry milling operation is also associated with the early formation of ZnO, as evinced by the XRD results. Possibly the oxide layer acts as a barrier and retards or prevents the alloying process.

3.2.2. Milling speed

A comparative study of wet milling of Cu₇₀Zn₃₀ blend at a B/P weight ratio of 10:1 in steel media, performed at different milling speeds of 200 and 300 r.p.m., showed a faster drop in crystallite size in the initial stage of milling in the later case (Fig. 7). However, the final crystallite size of α after 16 h milling was marginally lower at 200 r.p.m. It appears that there is an optimum energy for grinding at which the fracture and cold welding processes strike a balance to yield the finest crystallite size in a system.

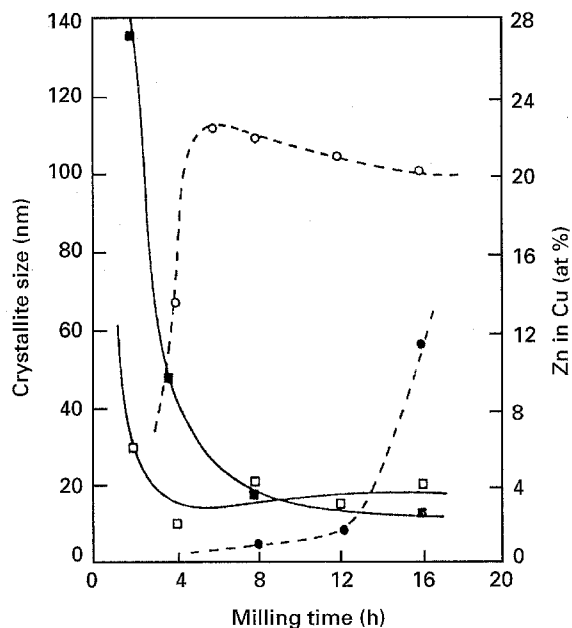


Figure 7 (□, ■) Crystallite refinement (—) and (○, ●) zinc content in α (---) (□, ○) as a function of time in $\text{Cu}_{70}\text{Zn}_{30}$ ball milled at (■, ●) 200 r.p.m. and (□, ○) 300 r.p.m.

3.2.3. Grinding medium

The contribution of the higher energy imparted by the WC medium is similar to that of higher milling speed, excepting the larger quantity of powder being employed in the former case for the same B/P ratio. Wet milling of $\text{Cu}_{70}\text{Zn}_{30}$ blend at a B/P weight ratio of 10:1 and a milling speed of 300 r.p.m. in WC media showed the formation of metastable strain-induced martensite within 1 h milling. Similar observation has been reported earlier [8] in the equiatomic blend. However, no such transformation could be detected in steel media. The higher specific gravity of WC as compared to steel imparts a higher energy to the powder particles and probably introduces larger strain in the system, sufficient to trigger the martensite formation. This martensite disappears during further milling possibly due to its compositional change. A much pronounced particle coarsening was observed in WC media after an initial drop in crystallite size (Fig. 8). This indicates more cold welding at higher milling energy. In $\text{Cu}_{70}\text{Zn}_{30}$ blend, a marginal increase in the maximum zinc content in α to ~23.3 at % (from 22 at % in the steel vial) was also achieved in the WC medium (Fig. 8) apparently due to the higher energy transfer during this milling.

4. Conclusions

1. Nanocrystalline α , β , γ and ϵ phases have been produced by mechanical alloying (MA) of elemental copper and zinc powders.

2. Irrespective of the starting composition of the blend, the zinc-rich phases (ϵ and γ) formed first during MA, possibly due to the much higher diffusivity of copper in zinc than vice versa.

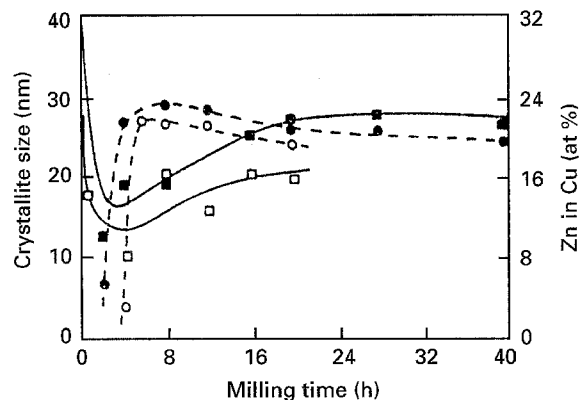


Figure 8 Change in (□, ■) crystallite size (—) and (○, ●) zinc content in α (---) (□, ○) steel and (■, ●) WC media at different milling times.

3. Rapid zinc-enrichment of α took place only after the α crystallite size reached about 15 nm.

4. After prolonged milling, the crystallite size of the copper-rich phase (α) was found to be much smaller than that in the zinc-rich phases (γ and ϵ), possibly due to the higher melting temperature of the former.

5. The dry milling showed slower alloying compared to wet milling, apparently due to the formation of oxide layers in the early stages of MA in the former.

6. Higher energy milling by means of a WC grinding medium showed more rapid alloying compared to that in steel media. Increase in the milling speed from 200 r.p.m. to 300 r.p.m. manifested similar enhancement in alloying.

Acknowledgement

The work was sponsored by the Department of Science and Technology, Government of India, Grant III.4(23) 92-ET.

References

1. E. HELLSTERN, H. J. FETCH, Z. FU and W. L. JOHNSON, *Mater. Res. Soc. Symp. Proc.* **132** (1989) 139.
2. B. S. MURTY, M. MOHAN RAO and S. RANGANATHAN, *Nanostruct. Mater.* **3** (1993) 459.
3. M. S. KIM and C. C. KOCH, *J. Appl. Phys.* **62** (1987) 3450.
4. B. S. MURTY, K. H. S. SINGH and S. K. PABI, *Bull. Mater. Sci.* **19** (1996) (3) in press.
5. B. S. MURTY, *Bull. Mater. Sci.* **16** (1993) 1.
6. C. C. KOCH, in "Processing of Metals and Alloys", edited by R. W. Cahn (VCH Publication, Weinheim, 1991) p.193.
7. A. R. YAVARI, *Mater. Sci. Eng.* **A179/A180** (1994) 20.
8. B. T. McDERMOTT and C. C. KOCH, *Scripta Metall.* **20** (1986) 669.
9. F. CARDELLINI, V. CONTINI, G. MAZZONE and M. VITTORI, *Scripta Metall. Mater.* **28** (1993) 1035.
10. B. D. CULLITY, "Elements of X-ray diffraction" (Addison Wesley, Massachusetts 1978) p.284.
11. A. GUINIER, "X-ray Diffraction" (Freeman, San Francisco, 1963) Massachusetts p.124.
12. W. B. PEARSON, "Lattice Spacing and Structure of Metals and Alloys" (Pergamon Press, Oxford, 1967) p.619.

13. R. M. DAVIS, B. T. McDERMOTT and C. C. KOCH, *Metall. Trans.* **19A** (1988) 2867.
14. R. B. SCHWARZ and C. C. KOCH, *Appl. Phys. Lett.* **49** (1986) 146.
15. R. C. WEAST, (ed.), "CRC handbook of chemistry and physics", 58th Edn (CRC Press, Ohio, 1977) p. F-62.
16. S. K. PABI, *Acta. Metall.* **27** (1979) 1693.
17. J. ECKERT, J. C. HOLZER, C. E. KRILL III and W. L. JOHNSON, *J. Mater. Res.* **7** (1992) 505.
18. C. C. KOCH, *Nanostruct. Mater.* **2** (1993) 109.

*Received 25 April
and accepted 7 November 1995*